

## Study the Effect of Rapid Thermal Annealing on Thin Films Prepared by Pulse Laser Deposition Method

Heba Salam Tareq

Applied Sciences Department, University of Technology/ Baghdad

Email: k\_zakria2000@yahoo.com

### ABSTRACT

In this paper, the synthesis of nanocrystalline Nickel oxide (NiO) thin films on quartz substrates using a pulsed 532 nm Q-Switched Nd: YAG laser is presented, the annealing temperature was varied from (200 - 400 °C). The X-ray diffraction (XRD) results show that the deposited films are crystalline in nature. Furthermore, a higher annealing temperature resulted in a thicker NiO film, which was attributed to an increased grain size. The morphology of deposited films were characterized by scanning electron microscope (SEM) and atomic force microscope (AFM); with increasing annealing temperature, the grain size increase. The grain size value (10,23 and 40 nm) for thin films annealing at 200, 300 and 400 °C respectively., and with increasing annealing temperature, surface roughness decrease. RMS roughness values were (13.5, 7.8 and 5.5 nm) for thin films annealing at 200, 300 and 400 °C respectively. UV-Vis spectrophotometric measurement showed high transparency (nearly 92 % in the wavelength range 400-900 nm) of the NiO thin film with a direct allowed band gap value lying in the range 3.51-3.6 eV.

**Keywords:** Nanostructure Nickel Oxide, Transparent Conducting Oxides, PLD.

### دراسة تأثير التلدين الحراري السريع على الاغشية الرقيقة المحضرة بطريقة الترسيب بالليزر النبضي

#### الخلاصة

في بحثنا هذا , تم تحضير اغشية رقيقة نانوية لأكسيد النيكل (NiO) على قواعد من الكوارتز باستخدام ليزر نيدميوم ياك النبضي ذو الطول الموجي (532 nm) , تغيرت درجة حرارة التلدين من (200-400) درجة مئوية . اظهرت نتائج حيود الاشعة السينية ان الاغشية المحضرة ذات طبيعة بلورية , كما ادى زيادة درجة حرارة التلدين الى زيادة بالحجم الحبيبي لاغشية اوكسيد النيكل. تم دراسة طوبوغرافية السطح باستخدام المجهر الالكتروني الماسح (SEM) ومجهر القوى الذرية (AFM) . بزيادة درجة حرارة التلدين ازداد الحجم الحبيبي. حيث تراوحت قيم الحجم الحبيبي لاغشية اوكسيد النيكل (10,23 و 40) نانومتر عند درجات حرارة تلدين (200, 300 و 400) مئوية على التوالي. ايضا" ادت زيادة درجة حرارة التلدين الى نقصان بخشونة السطح للاغشية المحضرة. حيث تراوحت قيم الخشونة لاغشية اوكسيد النيكل (13.5 , 7.8 و 5.5) نانومتر عند درجات حرارة تلدين (200, 300 و 400) مئوية على التوالي. كذلك تم دراسة الخصائص البصرية بواسطة مطياف النفاذية للأشعة المرئية وفوق البنفسجية. حيث اظهرت النتائج نفاذية أعلى من 92 % عند مدى الطول الموجي

(400-900) نانومتر لاغشية اوكسيد النيكل الرقيقة وتراوحت قيمة فجوة الطاقة للانتقال المباشر المسموح ( 3.51 - 3.6 ) الكترون فولت.

## INTRODUCTION

NiO is a well-known antiferromagnetic material [1], and a metal-deficient p-type semiconductor [2] with a 3.6 eV band gap [3]. Nickel oxide (NiO) films have a wide range of applications due to their excellent chemical stability. They have been used as catalysts [4], electrochromic display devices [5], fuel cells [6] and gas sensors [7]. NiO thin films usually exhibit p-type conductivity due to holes generated by Ni vacancies in the lattice and therefore NiO is an interesting candidate for materials research. Although structural and electrical properties of NiO films have been studied before, mechanical properties have been less investigated [8]. NiO thin films have been deposited by different techniques, including chemical self-assembling [9], sol-gel [10], RF sputtering [11], DC sputtering [12] and recently pulsed laser deposition (PLD) [13–15]. Preparation methods are essential for determining the microstructure and consequently the functional properties of synthesized structures.

In this work, pulsed laser deposition (PLD) was used for the deposition of NiO thin films at different annealing temperatures. The effect of annealing temperatures during deposition on the structural and optical properties was studied.

## EXPERIMENTAL DETAILS

Nickel oxide from ASDGF Company with a nickel target of 99.99% purity on glass slides as substrates. The powder was pressed less than 5 ton to form a target with 2.5 cm diameter and 0.4 cm thickness. Quartz slides each of 3 x 2 cm<sup>2</sup>. They were cleaned by alcohol with ultrasonic waves produced by Cerry PUL 125 device for 10 minutes in order to remove the impurities and residuals from their surfaces. Thin films were deposited using pulsed laser deposition by employing a Q-switched Nd: YAG laser at wavelength 532 nm with 0.4 J/cm<sup>2</sup> of energy density, pulse width 10 ns and repetition frequency 6 Hz. Uniform ablation ensured by rotating the target at constant speed shown in Figure (1). The focused Nd:YAG SHG Q-switching laser beam incident on the target surface making an angle of 45° with it. The films were deposited on quartz substrate at temperatures 300 °C. The pulsed laser deposition experiment was carried out inside a vacuum chamber generally in (10<sup>-2</sup> Torr) vacuum conditions. The substrates deposited at 100 °C temperature with NiO were annealed at 200 °C, 300 °C and 400 °C using a halogen lamp for 5 minute in air. The crystallinity of the prepared films was analyzed using X-ray Diffraction (XRD) measurements (Shimadzu 6000 made in Japan) using Cu K $\alpha$  radiation at 1.5406. and operating at an accelerating voltage of 40 kV and an emission current of 30 mA. Data were acquired over the range of 2 $\theta$  from 20° to 60°. The XRD method was used to study the change of crystalline structure. For morphological investigations, AFM images were recorded using Nanoscope scanning probe microscope controller in a tapping mode. The AFM images were used to observe the surface roughness and topography of deposited thin films and the surface morphology was examined by scanning electron microscopy (SEM-JEOL 7000). Optical measurements were conducted in the wavelength range 300 nm to 900 nm using a double beam UV-Visible spectrophotometer (UV-1650 UV-Visible Recording Spectrophotometer) Shimadzu made in Japan was used to measure the transmittance of NiO deposited. The transmittance data can be used to calculate absorption coefficients of the films at

different wavelength. Which have been used to determine the band gap  $E_g$ . The Film thickness measurements by optical interferometer method have been obtained.

## RESULTS AND DISCUSSION

### Structural properties

#### X-ray diffraction

The X-ray diffraction grams of films deposited on quartz substrates of different annealing temperatures are shown in Figure (2). The film deposited at 100 °C is poorly crystallized, but when we annealed the thin films at 200, 300 and 400 °C the peak centered at 33.4° according to the JCPDS 780643 is attributed to the (111) lattice plane reflection of the cubic NiO phase. The line peak at 46.9° corresponds to the (200) lattice plane reflection of the metallic Ni cubic phase [15], directly originating from the Ni target. The peak (311) at 67.2° may be due to a NiO compound, formed by diffusion in the film–substrate interface. Further research is necessary to clarify this issue.

At higher annealing temperature (400 °C), the intensity of the NiO peak increases and the grain size of nickel oxide grains increases with increasing annealing temperature.

The grain size of all NiO samples (2 0 0) diffraction line annealing at 200 °C to 400 °C was calculated using Scherer's equation and it is in the range of ~ (10, 23 and 40) nm, revealing a fine nanocrystalline grain structure. Can be seen in Table (1).

#### Atomic force microscopy (AFM)

The surface morphology of all the NiO films is presented by AFM images in tapping mode. The surface morphology reveals the Nano-crystalline NiO grains. Figure (3) shows the AFM images of the NiO thin films deposited at 100 °C and annealed at different temperatures (200, 300 and 400) °C. The surface morphology of the NiO thin films as observed from the AFM micrographs proves that the grains are uniformly distributed within the scanning area (10 μm x 10 μm). Annealing up to 200 °C impart a significant change in structure. The RMS roughness also decreased with increasing annealing temperatures. Annealing temperature certainly changes the topography drastically as shown in Table (2).

#### Scan electron microscope (SEM).

Figure (4) shows the SEM images of the NiO thin films deposited at 100 °C and annealing temperatures of (200, 300 and 400) °C respectively. NiO thin films have a quite uniform and hole-free surface. At (200, 300 and 400) °C annealing temperatures the film has homogeneous surface morphology. With increasing annealing temperature, the average size of aggregated particles increases. The grain size value (10, 23 and 40 nm) for thin films annealing at 200, 300 and 400 °C respectively it measured by use the program of the device as shown in Table (3).

#### Optical Properties

Figure (5) shows the transmittance spectra of NiO films. It is found that average transmittance of as-deposited NiO films is about 65% in the near-infrared region with respect to reference; It is obvious that the transmittance increases with the increase of annealing temperature. The blank glass substrate. Films annealed at 400 °C shows a significant increase in the range from 350nm to 900nm transmittance about 92 %. This is in consistent with the decrease of the surface roughness promoting the decrease of the surface scattering of the light [12]. Optical band gap was determined using the relation [11].

$$\alpha h\nu = A (h\nu - E_g)^r \quad \dots (1)$$

Where  $\alpha$  is the absorption coefficient,  $h\nu$  is the photon energy,  $E_g$  is the optical band gap,  $A$  is a constant which does not depend on photon energy and  $r$  has four numeric values (1/2 for allowed direct, 2 for allowed indirect, 3 for forbidden direct and 3/2 for forbidden indirect optical transitions). In this work, direct band gap was determined by plotting  $(\alpha h\nu)^2$  vs.  $h\nu$  curves, with the extrapolation of the linear region to low energies. From Figure (6), it was observed that direct optical band gap increases from 3.5 to 3.6 eV.

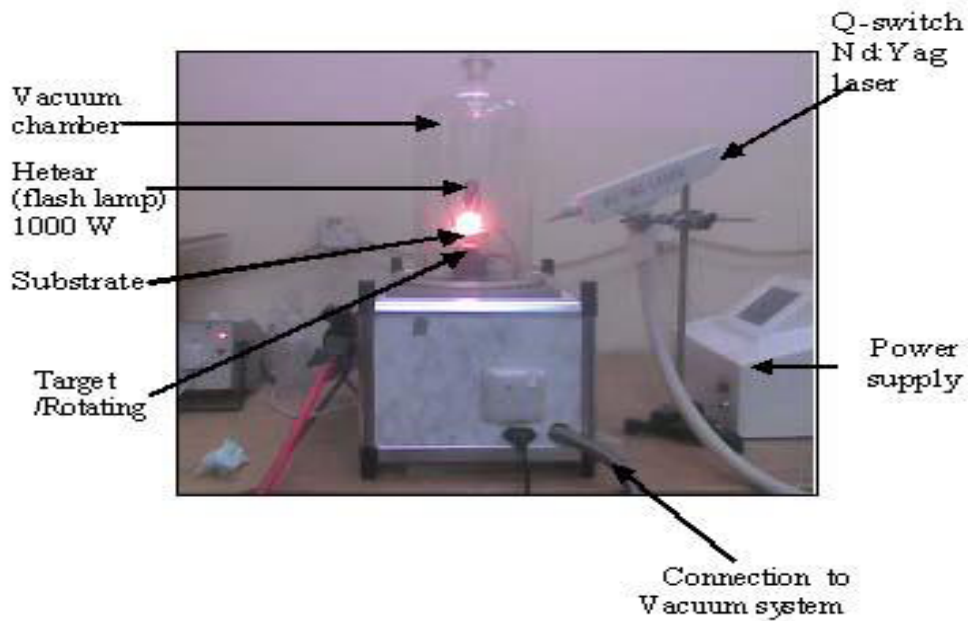


Figure (1) Experimental setup.

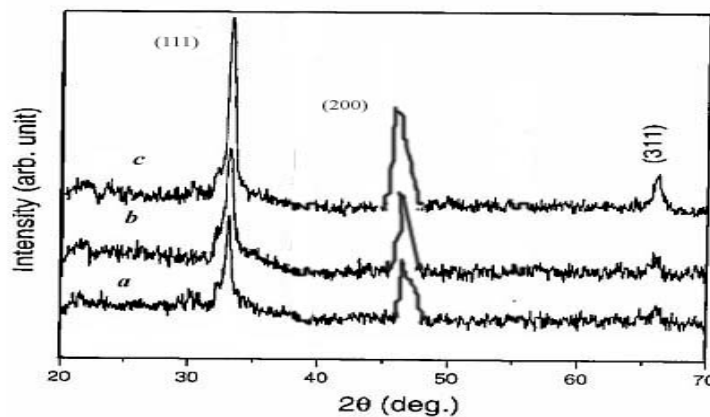


Figure (2) XRD patterns of a nanocrystalline NiO thin films deposited on quartz at different annealing temperature a) 200 C ,b) 300 C ,c) 400 C.

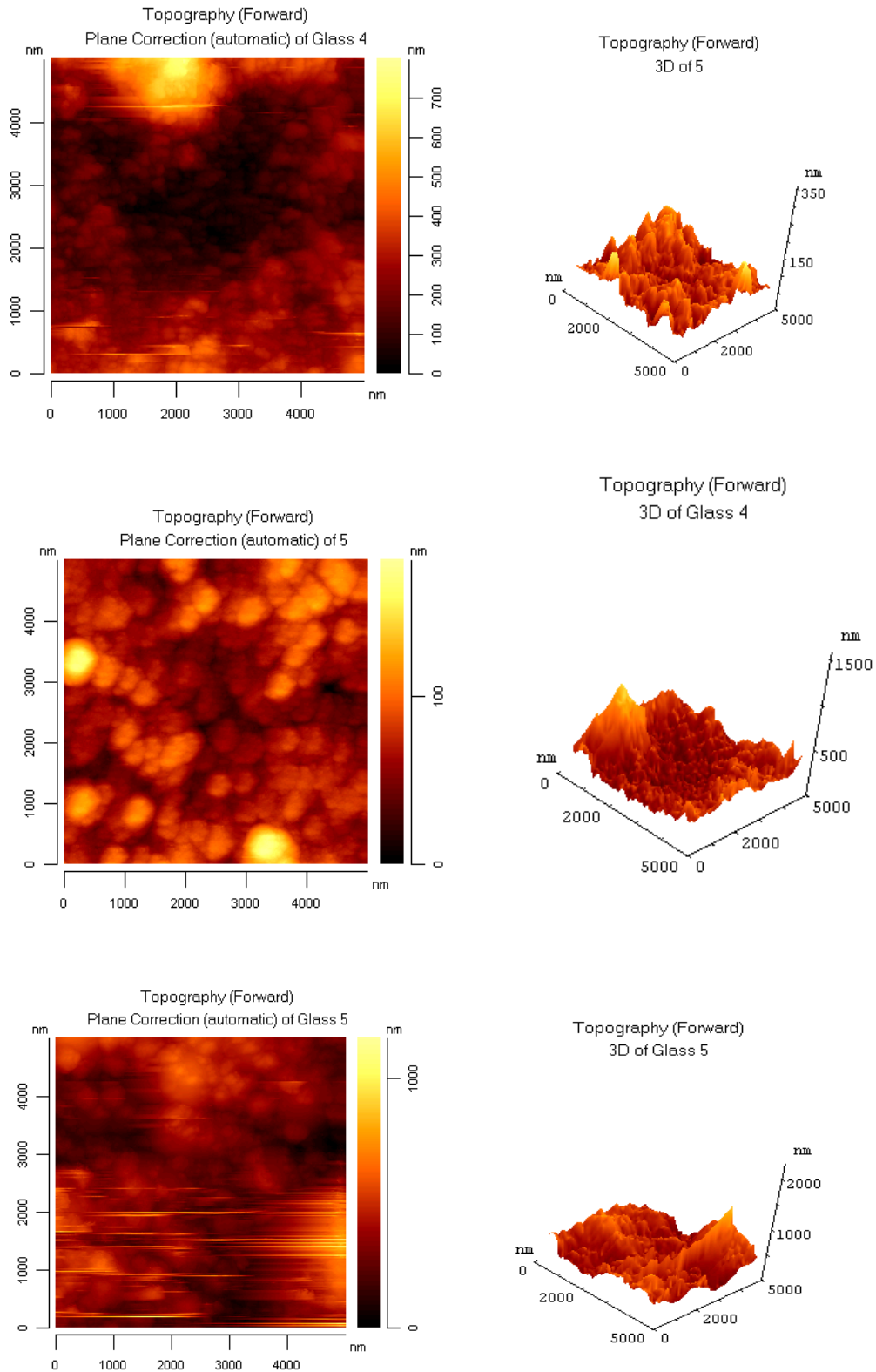


Figure (3) AFM image of patterns of a nanocrystalline NiO thin films deposited on quartz at different annealing temperature a) 200 C , b) 300 C , c) 400 C.

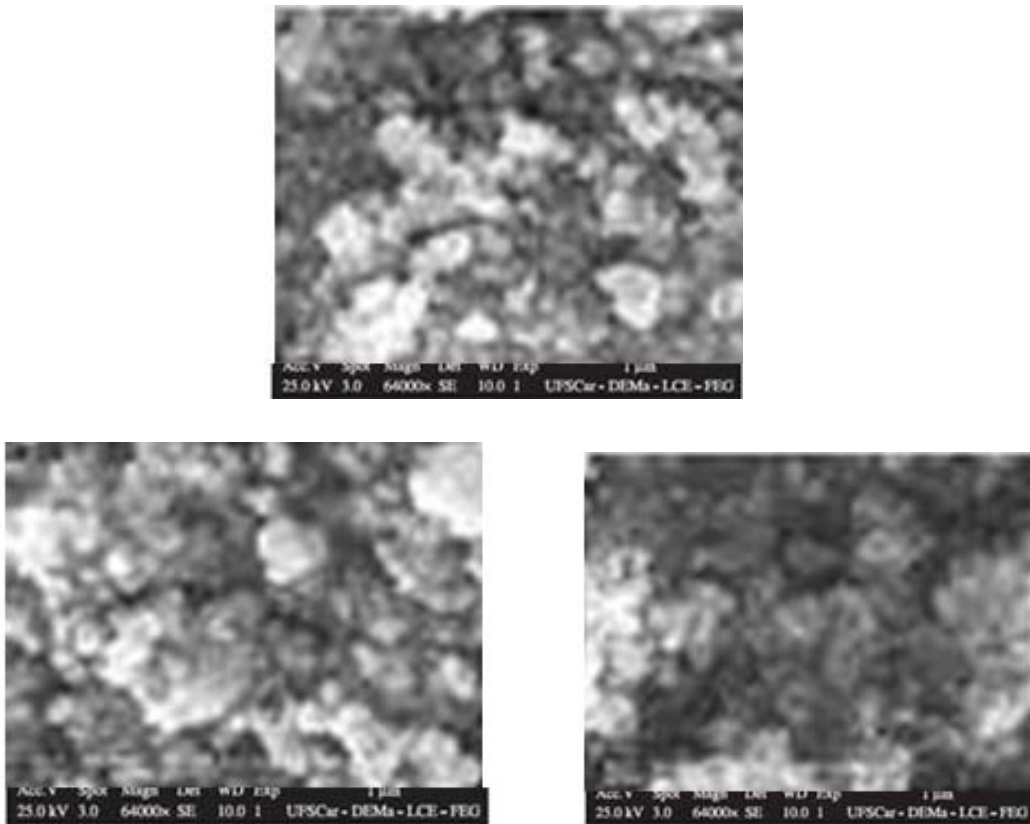


Figure (4) SEM image of patterns of a nanocrystalline NiO thin films deposited on quartz at different annealing temperature a) 200 C ,b) 300 C , c) 400 C.

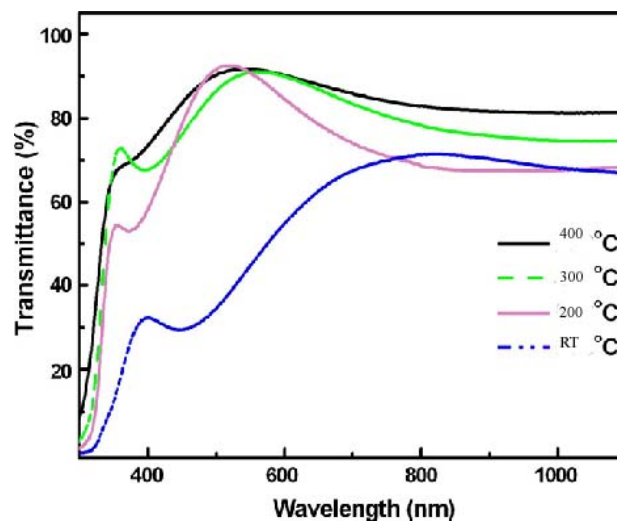


Figure (5) Transmittance spectra of a nanocrystalline NiO thin Films deposited on quartz at different annealing temperature.

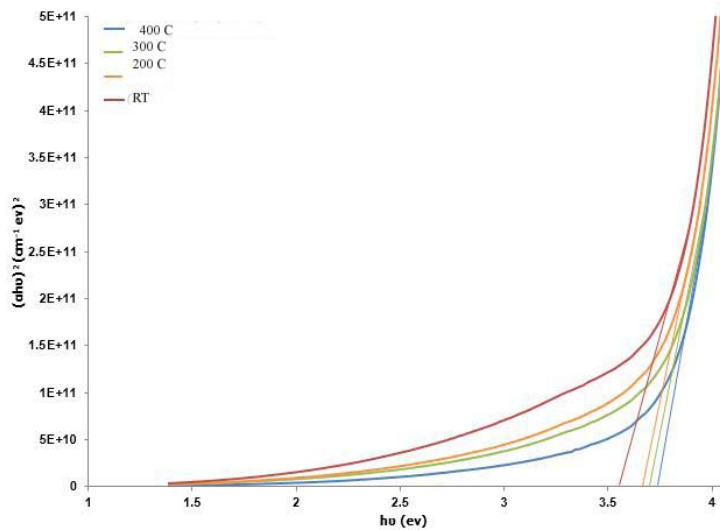


Figure (6) Variation of  $(ahv)^2$  versus energy curves of a nanocrystalline NiO thin films deposited on quartz at different annealing temperature .

Table (1) the obtained result of the structural parameters From XRD for NiO thin film.

$\square\square\square$ $\square$ degr ee)	(hkl)	Lattice constant Å	FWHM M'	Main grain size (nm)
46.9	(200)	9.41	0.65	26.28
46.9	(200)	9.41	0.5	33.6
46.9	(200)	9.42	0.33	46.88

Table (2) Morphological characteristics from AFM Images for NiO thin film.

sample	RMS roughness(nm)
NiO As deposited	20
NiO annealing at 200 °C	13.5
NiO annealing at 300 °C	7.8
NiO annealing at 400 °C	5.5

**Table (3) Morphological characteristics from SEM  
Images for NiO thin film.**

<i>sample</i>	<i>SEM of plane grain size (nm)</i>
<b>NiO As deposited</b>	<b>8</b>
<b>NiO annealing at 200 °C</b>	<b>10</b>
<b>NiO annealing at 300 °C</b>	<b>23</b>
<b>NiO annealing at 400 °C</b>	<b>40</b>

**CONCLUSIONS**

Nanostructured Nickel oxide thin films were prepared by pulsed laser deposition techniques on the quartz substrate. The effect of annealing temperature on structure, morphology and optical properties of NiO thin films were studied by XRD, AFM, SEM and UV-Visible measurements. The XRD results reveal that the deposited thin film and annealed at 400 °C of NiO have a good Nan crystalline (high intensity). At higher annealing temperature (400 °C), the intensity of the NiO peak increases and the grain size of nickel oxide grains increases with increasing annealing temperature. With increasing annealing temperature, the average size of aggregated particles increases. The AFM results showed the slow growth of crystallite sizes for the as-grown films and annealed films from 200 to 400 °C, and the RMS roughness also decreased with increasing annealing temperatures. The transmittance increased with increasing annealing temperature. The film annealed at 400 °C has the highest transmittance among the films. It is observed that the allowed direct optical band gap of the films increases from 3.5 to 3.6 eV.

**REFERENCES**

- [1]. Fujii, E. A. Tomozawa, H. Torii, and R. Takayama, Japanese Journal of Applied Physics 35 (1996) L328.
- [2]. Sato, H. T. Minami, S. Takata, and T. Yamada, Thin Solid Films 236 (1993) 27.
- [3]. Sasi, B. K.G. Gopchandran, P.K. Manoj, P. Koshy, P. Prabhakara Rao, and V.K. Vaidyan, Vacuum 68 (2003) 149.
- [4]. Roslik, A.K. V.N. Konev, and A.M. Maltsev, Oxidation of Metals 43 (1995) 1.
- [5]. Ahn, K.S. Y.C. Nah, and Y.E. Sung, Applied Surface Science 199 (2002) 259.
- [6]. Chen, X. N.J. Wu, L. Smith, and A. Ignatiev, Applied Physical Letters 84 (2004) 2700.
- [7]. Fasaki, I. A. Giannoudakos, M. Stamataki, M. Kompitsas, E. Gyorgy, I.N. Mihailescu, F. Roubani-Kalantzopoulou, A. Lagoyannis, and S. Harissopulos, Applied Physics A 91 (2011) 487.
- [8]. Huntz, A.M. M. Andrieux, and R. Molins, Materials Science and Engineering A 417 (2006) 8.
- [9]. Souza Cruz, Y. Wang, C. Ma, X. Sun, and H. Li, Microporous Mesoporous Materials 71 (2004) 99.
- [10]. Jiao, Z. M. Wu, Z. Qin, and H. Xu, Nanotechnology 14 (2012) 458.
- [11]. Souza Cruz, T.G. and M.U. Hleinke, A. Gorenstein, Applied Physics Letters 81 (2002) 4922.

- [12] M. Lee, S. Seo, D. Seo, E. Jeong, and I.K. Yoo, *Integrated Ferroelectrics* 68 (2012) 19.
- [13]. Zbroniec, L. T. Sasaki, N. Koshizaki, *Journal of Ceramic Processing Research* 6 (2005) 134.
- [14]. Sasi, B. and K.G. Gopchandran, *Nanotechnology* 18 (2013) 115613.
- [15]. Stamataki, M. D. Tsamakis, N. Brilis, I. Fasaki, A. Giannoudakos, and M. Kompitsas, *Physica Status Solidi A-Applied Research* 205 (2008) 2064–20